High resolution time-to-space conversion of sub-picosecond pulses at 1.55μm by non-degenerate SFG in PPLN crystal

Dror Shayovitz[1,*] Harald Herrmann,[2] Wolfgang Sohler,[2] Raimund Ricken,[2] Christine Silberhorn,[2] and Dan M. Marom[1]

[1]*Department of Applied Physics, Hebrew University of Jerusalem, Jerusalem, 91904, Israel*
[2]*Department of Applied Physics, The University of Paderborn, Warburger Str. 100 D-33098, Paderborn, Germany*
[*]*dror.shayovitz@mail.huji.ac.il*

Abstract: We demonstrate high resolution and increased efficiency background-free time-to-space conversion using spectrally resolved non-degenerate and collinear SFG in a bulk PPLN crystal. A serial-to-parallel resolution factor of 95 and a time window of 42 ps were achieved. A 60-fold increase in conversion efficiency slope compared with our previous work using a BBO crystal [D. Shayovitz and D. M. Marom, Opt. Lett. **36**, 1957 (2011)] was recorded. Finally the measured 40 GHz narrow linewidth of the output SFG signal implies the possibility to extract phase information by employing coherent detection techniques.

OCIS codes: (190.0190) Nonlinear optics; (320.0320) Ultrafast optics; (060.0060) Fiber optics and optical communications.

References and links

1. T. Richter, E. Palushani, C. Schmidt-Langhorst, R. Ludwig, L. Molle, M. Nolle, and C. Schubert, "Transmission of single-channel 16-QAM data signals at terabaud symbol rates," J. Lightwave Technol. **30**(4), 504–511 (2012).
2. B. C. Wang, V. Baby, W. Tong, L. Xu, M. Friedman, R. J. Runser, I. Glesk, and P. R. Prucnal, "A novel fast optical switch based on two cascaded Terahertz Optical Asymmetric Demultiplexers (TOAD)," Opt. Express **10**(1), 15–23 (2002).
3. H. Le Minh, Z. Ghassemlooy, and W. Pang Ng, "Characterization and performance analysis of a TOAD switch employing a dual pulse scheme in high-speed OTDM demultiplexer," IEEE Commun. Lett. **12**(4), 316–318 (2008).
4. J. Du, Y. Dai, G. K. P. Lei, and C. Shu, "Reconfigurable two-channel demultiplexing using a single baseband control pulse train in a dispersion asymmetric NOLM," Opt. Express **18**(18), 18691–18696 (2010).
5. K. I. Kang, I. Glesk, T. G. Chang, P. R. Prucnal, and R. K. Boncek, "Demonstration of all-optical Mach-Zehnder demultiplexer," Electron. Lett. **31**(9), 749–750 (1995).
6. T. Miyazaki and F. Kubota, "Simultaneous demultiplexing and clock recovery for 160-Gb/s OTDM signal using a symmetric Mach-Zehnder switch in electrooptic feedback loop," IEEE Photon. Technol. Lett. **15**(7), 1008–1010 (2003).
7. T. Hirooka, M. Okazaki, T. Hirano, P. Guan, M. Nakazawa, and S. Nakamura, "All-optical demultiplexing of 640-Gb/s OTDM-DPSK signal using a semiconductor SMZ switch," IEEE Photon. Technol. Lett. **21**(20), 1574–1576 (2009).
8. E. S. Awad, P. S. Cho, N. Moulton, and J. Goldhar, "All-optical timing extraction with simultaneous opyical demultiplexing from 40 Gb/s using a single electroabsorption modulator," IEEE Photon. Technol. Lett. **15**(1), 126–128 (2003).
9. A. Cheng, M. P. Fok, and C. Shu, "All-optical tunable delay line for channel selection in OTDM demultiplexing," in *Asia Optical Fiber Communication and Optoelectronic Exposition and Conference*, OSA Technical Digest (CD) (Optical Society of America, 2008), paper SuA3. *http://www.opticsinfobase.org/abstract.cfm?URI=AOE-2008-SuA3*
10. F. Li, M. Pelusi, D.-X. Xu, A. Densmore, R. Ma, S. Janz, and D. J. Moss, "Error-free all-optical demultiplexing at 160Gb/s via FWM in a silicon nanowire," Opt. Express **18**(4), 3905–3910 (2010).
11. B. Corcoran, M. D. Pelusi, C. Monat, J. Li, L. O'Faolain, T. F. Krauss, and B. J. Eggleton, "Ultracompact 160 Gbaud all-optical demultiplexing exploiting slow light in an engineered silicon photonic crystal waveguide," Opt. Lett. **36**(9), 1728–1730 (2011).
12. C. Koos, P. Vorreau, T. Vallaitis, P. Dumon, W. Bogaerts, R. Baets, B. Esembeson, I. Biaggio, T. Michinobu, F. Diedrich, W. Freude, and J. Leuthold, "All-optical high-speed signal processing with silicon-organic hybrid slot waveguides," Nat. Photonics **3**(4), 216–219 (2009).

#175578 - $15.00 USD Received 5 Sep 2012; revised 27 Oct 2012; accepted 28 Oct 2012; published 19 Nov 2012

13. M. Galili, J. Xu, H. C. Mulvad, L. K. Oxenløwe, A. T. Clausen, P. Jeppesen, B. Luther-Davis, S. Madden, A. Rode, D.-Y. Choi, M. Pelusi, F. Luan, and B. J. Eggleton, "Breakthrough switching speed with an all-optical chalcogenide glass chip: 640 Gbit/s demultiplexing," Opt. Express **17**(4), 2182–2187 (2009).
14. R. Takahashi, T. Yasui, J. Seo, and H. Suzuki, "Ultrafast all-optical serial-to-parallel convertors based on spin-polarized surface-normal optical switches," IEEE J. Sel. Top. Quantum Electron. **13**(1), 92–103 (2007).
15. T. Nakahara, H. Takenouchi, R. Urata, H. Yamazaki, and R. Takahashi, "Hybrid optoelectronic buffer using CMOS memory and optical interfaces for 10-Gbit/s asynchronous variable-length optical packets," Opt. Express **18**(20), 20565–20571 (2010).
16. Y. Oshita, T. Konishi, and Y. Ichioka, "Ultrafast time-to-two-dimensional-space conversion system usng SHG crystal," Opt. Rev. **9**(4), 141–145 (2002).
17. Y. Oshita, T. Konishi, W. Yu, K. Itoh, and Y. Ichioka, "Application of ultrafast time-to-two-dimensional-space-to-time conversion (II): time-varying spectral control for arbitrary ultrafast signal reshaping," IEEE Photon. Technol. Lett. **16**(2), 623–625 (2004).
18. M. A. Foster, R. Salem, D. F. Geraghty, A. C. Turner-Foster, M. Lipson, and A. L. Gaeta, "Silicon-chip-based ultrafast optical oscilloscope," Nature **456**(7218), 81–84 (2008).
19. K. G. Petrillo and M. A. Foster, "Scalable ultrahigh-speed optical transmultiplexer using a time lens," Opt. Express **19**(15), 14051–14059 (2011).
20. E. Palushani, H. C. Hansen Mulvad, M. Galili, H. Hu, L. K. Oxenlowe, A. T. Clausen, and P. Jeppesen, "OTDM-to-WDM conversion based on time-to-frequency mapping by time-domain optical Fourier transformation," IEEE J. Sel. Top. Quantum Electron. **18**(2), 681–688 (2012).
21. H. Hu, J. Yu, L. Zhang, A. Zhang, W. Wang, J. Wang, Y. Jiang, and E. Yang, "40Gb/s all-optical serial-to-parallel conversion based on a single SOA," IEEE Photon. Technol. Lett. **20**(13), 1181–1183 (2008).
22. P.-C. Sun, Y. T. Mazurenko, and Y. Fainman, "Femtosecond pulse imaging: ultrafast optical oscilloscope," J. Opt. Soc. Am. A **14**(5), 1159–1170 (1997).
23. A. M. Kan'an and A. M. Weiner, "Efficient time-to-space conversion of femtosecond optical pulses," J. Opt. Soc. Am. B **15**(3), 1242–1245 (1998).
24. D. M. Marom, D. Panasenko, P.-C. Sun, and Y. Fainman, "Linear and nonlinear operation of a time-to-space processor," J. Opt. Soc. Am. A **18**(2), 448–458 (2001).
25. J.-H. Chung and A. M. Weiner, "Real-time detection of femtosecond optical pulse sequences via time-to-space conversion in the lightwave communications band," J. Lightwave Technol. **21**(12), 3323–3333 (2003).
26. D. Shayovitz and D. M. Marom, "High-resolution, background-free, time-to-space conversion by collinearly phase-matched sum-frequency generation," Opt. Lett. **36**(11), 1957–1959 (2011).
27. D. Shayovitz, H. Herrmann, W. Sohler, R. Ricken, C. Silberhorn, and D. M. Marom, "High resolution time-to-space conversion of sub-picosecond pulses at 1.55μm by non-degenerate SFG in PPLN crystal," in *Nonlinear Photonics,* OSA Technical Digest (online) (Optical Society of America, 2012), paper NM3C.2. *http://www.opticsinfobase.org/abstract.cfm?URI=NP-2012-NM3C.2*

1. Introduction

Optical communications networks are subject to ever increasing capacity demands due to the rapid growth in internet traffic. Two principle approaches in support of these demands are increasing parallelism using wavelength division multiplexing (WDM), filling the gain bandwidth of optical amplifiers, and increasing bandwidth efficiency using advanced modulation formats such as phase-shift keying (PSK). WDM channel reduction is desirable and may be enabled by boosting the serial transmission rate to higher baud rates. This can be achieved by optical time division multiplexing (OTDM) where short pulses are electrooptically modulated at relatively low bandwidths (10's of GHz) and then interleaved into a single high speed serial channel using passive optical delay lines. A recent demonstration of 10.2 Tbit/s data transmission achieved by 1.28 Tbaud/s multiplexing together with 16-QAM (quadrature amplitude modulation) [1] underlines the potential of OTDM for maximizing single wavelength channel data capacity by combining a high symbol rate and multiple bits-per-symbol modulation.

Whilst generating the OTDM channel is relatively straightforward, detection after transmission is more challenging. Direct or coherent optoelectronic detection of terabaud OTDM is not possible due to electric circuit bandwidth limitations. Generally all-optical demultiplexing using a fast nonlinear optical interaction is required; examples include the nonlinear optical loop mirror switch [2–4], the semiconductor optical amplifier based Mach-Zehnder switch [5–7], cross-absorption modulation [8,9] and four-wave mixing in silicon, silicon-organic hybrid or chalcogenide $\chi^{(3)}$ nonlinear waveguides [10–13]. While each technique has its own advantages and disadvantages, their operation principles limit them to single sub-channel (tributary) extraction from the OTDM channel. The result is that the number of devices required to fully demultipex the incoming data stream, and hence also

#175578 - $15.00 USD Received 5 Sep 2012; revised 27 Oct 2012; accepted 28 Oct 2012; published 19 Nov 2012

power consumption, scales with the OTDM channel baud rate. The need for multiple devices leads to the even more serious problem of inter-device timing synchronization, which becomes critical at rates of 100's Gbaud/s and higher.

These problems can be overcome using serial-to-parallel conversion where a single device simultaneously demultiplexes all tributaries out of the OTDM channel, resulting in parallel lower bandwidth output channels which can then be detected optoelectronically. Examples include multiple quantum well based time-to-space conversion [14, 15], angle phase-matched time-and-frequency-to-two-dimensional-space conversion [16, 17], time-to-frequency conversion based on four-wave mixing [18–20] or semiconductor optical amplifier based cross-phase modulaton [21] and spectrally resolved sum-frequency generation (SFG) time-to-space conversion [22–27]. Serial-to-parallel demultiplexing avoids the problem of inter-device clock synchronization and is robust against detection errors due to timing jitter in the transmitted pulse stream.

In this paper we present spectrally resolved SFG time-to-space (T-S) conversion for serial-to-parallel demultiplexing using a bulk periodically-poled lithium niobate (PPLN) crystal. This technique converts a fast temporal data stream to a quasi-static spatial image which can then be detected by an array of photodetectors. In addition to relief from precise timing synchronization, an advantage of T-S conversion is the preservation of phase information during the conversion process and the generation of a narrowband output signal. This characteristic makes T-S conversion especially attractive when compared to time-to-frequency conversion, which generates a wideband output signal making coherent detection inaccessible. Other serial-to-parallel conversion techniques mentioned above (multiple quantum well based T-S conversion and angle phase-matched time-and-frequency-to-two-dimensional-space conversion) are limited, respectively, in speed by the picosecond scale charge carrier lifetime and in conversion efficiency by the non-collinearly phase-matched interaction and requirement for one gating pulse per demultiplexed signal pulse.

Spectrally resolved T-S conversion using second harmonic generation (SHG) was first demonstrated in a lithium triborate crystal at 920 nm [22]. Collinear non-critically phase-matched degenerate SHG at 860 nm in potassium niobate [23] resulted in improved conversion efficiency, but without the possibility of filtering out the background light. T-S conversion at 1560 nm (i.e. in the optical communications C-band) in PPLN was demonstrated [25]. However a limited time window of 25 ps was obtained due to the large spectral component focused spot size necessary for the long interaction length required to obtain the reported conversion efficiency of 0.6%. Non-degenerate, collinearly phase-matched SFG for background-free T-S conversion in the telecom window using a beta barium borate (BBO) crystal was recently demonstrated, with high resolution but low conversion efficiency due to the relatively small nonlinear coefficient of BBO [26]. Here we provide an updated summary of our research on T-S conversion with PPLN presented at the OSA Topical Meeting on Nonlinear Photonics (Colorado Springs, 17-21 June 2012) [27]. In particular, we employ a custom made wide aperture PPLN chip to achieve increased conversion efficiency whilst preserving high resolution and background-free operation. Additionally, the effect of T-S conversion with non-degenerate SFG on the time-to-space mapping factor is determined and experimentally verified, and an approach to achieve higher conversion efficiency by means of a PPLN planar waveguide is proposed.

2. Non-degenerate time-to-space conversion

Time-to-space conversion is based on SFG between the dispersed frequency components of a signal pulse stream and a single reference pulse in a nonlinear medium [22, 24] (see Fig. 1). The signal and reference beams, at central frequencies ω_s and ω_r respectively, are incident on different diffraction gratings and then pass through a Fourier lens, such that their resolved spectra are superimposed at the focal plane with equal magnitude and opposite direction linear spatial dispersions. By placing a $\chi^{(2)}$ nonlinear crystal at this plane SFG occurs between the overlapping frequency components at each point in space. Due to the matched yet flipped spatial dispersions a quasi-monochromatic SFG wave is generated at each location along the

#175578 - $15.00 USD Received 5 Sep 2012; revised 27 Oct 2012; accepted 28 Oct 2012; published 19 Nov 2012

crystal aperture, with automatic phase-matching across the whole bandwidth of the dispersed pulses. In addition the problem of temporal walkoff associated with short pulse harmonic generation is avoided, since the spectrally resolved pulses are stretched in time.

The generated SFG light carries an instantaneous linear spatial phase which is directly dependant on the time delay between the interacting signal and reference pulses. A second Fourier lens placed after the crystal converts this spatial phase into a transverse spatial shift of the focused pulse image at the output plane. The result is a slowly varying spatial image of the input waveform with one-to-one mapping of the time delay, Δt, of the incoming pulses to a spatial shift, Δx, of the output image. Each spatial pulse image corresponds to a single OTDM bit slot and so may be directly detected by a photodetector or mixed with a narrow linewidth local oscillator for coherent detection.

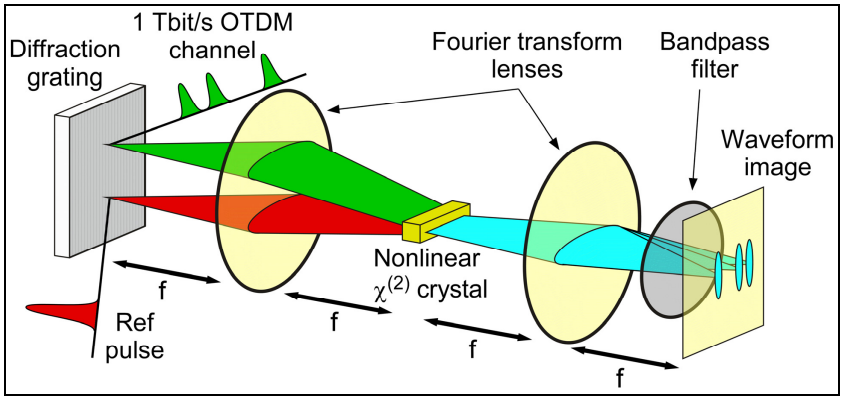

Fig. 1. Time-to-space conversion concept. The time domain information carried by an OTDM channel is transferred to a space domain image via dispersed wave SFG, enabling direct or coherent detection. Note that a non-collinear phase-matching configuration is shown here for clarity, whereas the current experiment utilizes collinear phase-matching for an extended interaction length, necessitating the use of a bandpass filter for separating the SFG light from the background SHG of the signal and reference beams.

The time-to-space mapping factor is given by the product of the linear spatial dispersion and a scaling factor incorporating the new carrier frequency due to the second spatial Fourier transform [25]; taking into account the non-degenerate wavelengths of our signal and reference pulses results in:

$$\frac{\Delta x}{\Delta t} = \frac{f_2}{f_1} \cdot \frac{c \cos \beta}{f_{g,s} \lambda_s} \cdot \frac{\lambda_r}{\lambda_s + \lambda_r} \tag{1}$$

where f_1 and f_2 are the focal lengths of the first and second Fourier lenses respectively, c is the speed of light, β is the angle of diffraction of the central wavelength component of the dispersed signal pulse, $f_{g,s}$ is the signal pulse diffraction grating frequency and λ_s and λ_r are the signal and reference pulse central wavelengths respectively. Equation (1) reduces to the same scaling factor presented in [25] for the degenerate case.

In addition to the information carrying SFG signal at $\omega_s + \omega_r$, the signal and reference pulses each independently produce SHG light centered about $2\omega_s$ and $2\omega_r$. This light carries no useful information, yet propagates to the output spatial image plane and there forms an unwanted background to the pulse image. However, since the interacting pulses are at non-degenerate wavelengths the SHG background light is spectrally offset from the SFG signal (ie. $2\omega_s > \omega_s + \omega_r > 2\omega_r$), and so a background-free output image can be obtained by placing a bandpass spectral filter centered about $\omega_s + \omega_r$. This also allows the use of collinearly propagating signal and reference beams, thus maximizing their interaction length inside the nonlinear medium.

#175578 - $15.00 USD Received 5 Sep 2012; revised 27 Oct 2012; accepted 28 Oct 2012; published 19 Nov 2012

The key performance metrics of the T-S converter are the serial-to-parallel resolution factor, N, and the conversion efficiency, η. The resolution factor N determines the maximum number of signal pulses that can be simultaneously demultiplexed by a single reference pulse and is dependent on the time window of operation. The limited time window stems from the decrease in output image intensity due to less temporal overlap with increasing time delay between the reference pulse and a signal pulse at the $\chi^{(2)}$ nonlinear crystal.

The conversion efficiency η is defined as the SFG output power divided by the signal beam power incident on the nonlinear crystal. The resolution-efficiency product is invariant to the spot size of a spectral component focused at the crystal, so that one parameter can be improved at the expense of the other [24]. In other words, decreasing the spectral component spot size results in an enhanced resolution, but this is achieved at the expense of conversion efficiency due to the shorter interaction length. However the larger $\chi^{(2)}$ nonlinearity of PPLN compared with BBO allows an increase in conversion efficiency without loss of resolution.

3. Experiment

Our experimental setup is shown in Fig. 2. The signal and idler (reference) outputs of a Spectra-Physics Opal OPO (with signal pulse duration 100 fs and repetition rate 80.2 MHz) are expanded to appropriate collimated beam sizes and undergo equal and opposite linear spatial dispersions of approximately 5 mm over a 40 nm (FWHM) bandwidth by diffraction gratings and 75 mm lenses. The dispersed beams are superimposed by a dichroic mirror and are incident on a PPLN crystal located at the focal plane. The main characteristics of the input beams are given in Table 1. Noncritically phase-matched SFG results in a quasi-monochromatic output beam at 810 nm, which another lens of focal length 75 mm coherently focuses to a tight spot at the pulse image plane. A CMOS camera records the output spatial image, with background second harmonic light from the signal and reference beams being blocked by a bandpass filter between the lens and the camera.

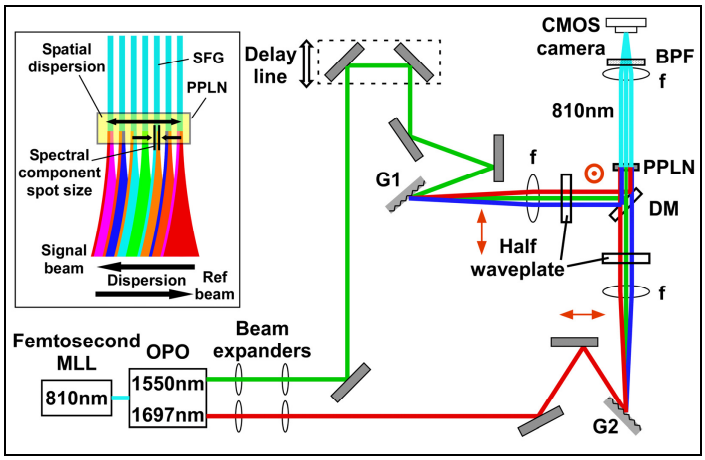

Fig. 2. Experimental setup (MLL, mode-locked laser; OPO, optical parametric oscillator; G1/G2, grating; f, Fourier lens; DM, dichroic mirror; PPLN, periodically-poled lithium niobate; BPF, bandpass filter. Inset: dispersed signal and reference beams at the PPLN chip.

Table 1. Input Beam Characteristics of Time-to-Space Converter[a]

	λ_0 (nm)	f_g (lp/mm)	α (°)	β (°)	dx/dv (mm/THz)	w_0 (μm)	P_{av}/P_{max} (mW/kW)
Signal	1550	1100	70	50	1.03	13	240/30
Reference	1697	1000	80	45	−1.03	14	64/8

[a]λ_0, central wavelength; f_g, grating frequency; α, incidence angle on grating; β, diffraction angle of central wavelength component; dx/dv, spatial dispersion; w_0, focused spot radius of single spectral component in the horizontal direction; Pav/Pmax; average beam power/peak power at the PPLN. Ideally the reference beam power would be higher than the signal power.

#175578 - $15.00 USD Received 5 Sep 2012; revised 27 Oct 2012; accepted 28 Oct 2012; published 19 Nov 2012

PPLN was chosen as the nonlinear medium due to its high d_{eff} coefficient of 16 pm/V (taking into account the reduction by a factor $2/\pi$ due to periodic poling) and the absence of spatial walkoff between the extraordinary polarized interacting beams. The PPLN chip used in this experiment was fabricated and anti-reflection coated, with a domain length of 20.3 μm (for a phase-matching temperature of 165 °C) and dimensions of 6 mm in the light propagation direction and 10 mm in the spatial dispersion direction. The extra wide crystal aperture is necessary in order to accommodate the full spatial extent of the dispersed beams and avoid limiting the interaction bandwidth. The confocal length of the focused spectral components of the signal and reference beams in the plane of dispersion was 1.5 mm, thus only a short section of the crystal length is utilized in practice.

4. Results

An example pulse image with a sech squared fit to its horizontal cross-section is shown in Fig. 3(a); we placed a neutral density filter in front of the camera in order to suppress saturation. By varying the delay line in the signal beam path the temporal offset between the signal and reference pulses arriving at the PPLN is controlled. This temporal offset is translated by the T-S conversion process into a transverse spatial shift of the pulse image. Inserting the experimental setup parameters (see Table 1) into Eq. (1) gives a T-S conversion factor of 59.1 μm/ps, in excellent agreement with the measured conversion factor of 58.8 μm/ps. In order to demonstrate the potential for demultiplexing a 1 Tbit/s OTDM channel we recorded 42 individual pulse images at 1 ps separation throughout the FWHM time window (Figs. 3(b) and 3(c)).

The time window was determined by measuring the variation in output pulse image intensity with time delay and the conversion efficiency was measured using a power meter placed after the bandpass filter (at zero time delay); the results are summarized in Table 2.

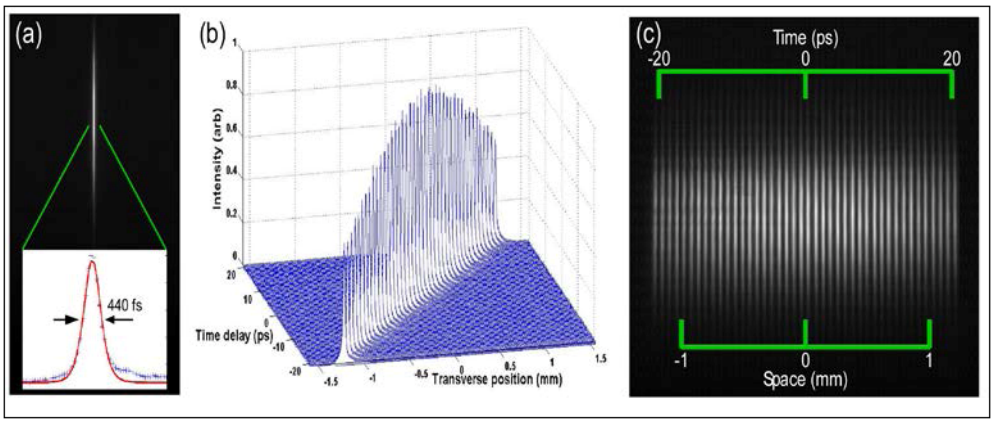

Fig. 3. (a) T-S converted signal pulse image with 440 fs FWHM, (b) pulse image intensity profiles showing shift in spatial position and intensity fall-off with varying time delay and (c) 42 pulse images distributed throughout the T-S processor time window (composite image).

Table 2. PPLN-based T-S Conversion Performance Parameters[a]

ΔT (ps)	τ (fs)	N (= ΔT/ τ)	η (%)	Conversion efficiency slope (%/W)	Bandwidth (nm)
42	440	95	0.03	0.6	0.09

[a]ΔT, FWHM time window; τ, FWHM pulse image width; N, serial-to-parallel resolution factor; η, conversion efficiency.

Note that the pulse image width at 440 fs is approximately three times longer than the expected width for the 100 fs signal pulse (including the autocorrelation factor of ~1.5). This is mainly due to the fact that our reference pulse duration is 210 fs. Of course the reference pulse should ideally be short and intense compared to the signal pulse, enabling high T-S

#175578 - $15.00 USD Received 5 Sep 2012; revised 27 Oct 2012; accepted 28 Oct 2012; published 19 Nov 2012

fidelity and conversion efficiency. A factor 30 increase in conversion efficiency and factor 60 increase in conversion efficiency slope compared with our previous work using BBO [26] were achieved (see Fig. 4(a)). This compares well with the predicted increase in conversion efficiency slope due to the larger nonlinear coefficient of PPLN:

$$\frac{\eta_{SFG-PPLN}}{\eta_{SFG-BBO}} = \left(\frac{(2/\pi) \cdot d_{eff,LiNbO3}}{d_{eff,BBO}} \right)^2 = 64 \qquad (2)$$

where η is conversion efficiency and d_{eff} is the effective nonlinear coefficient of the crystal.

Finally, the SFG bandwidth was measured as 0.09 nm using light coupled by a single mode fiber into an optical spectrum analyzer (Fig. 4(b)). This two order-of-magnitude reduction from the input signal bandwidth (5 THz to 40 GHz) brings the ultrafast input waveform to within the detection bandwidth of a fast optoelectronic receiver. In addition, the relatively narrow linewidth of the converted signal shows the potential for extraction of phase information using coherent detection.

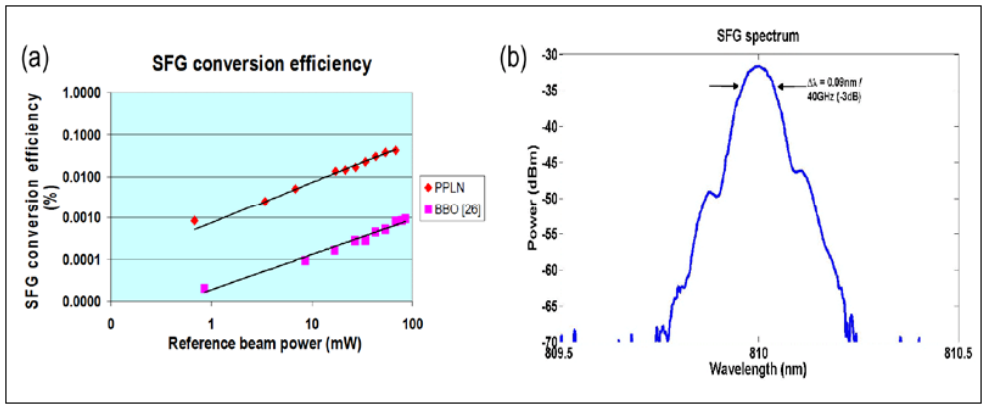

Fig. 4. (a) T-S conversion efficiency slope with PPLN (red diamonds) and BBO (pink squares) and (b) SFG narrowband spectrum centered at 810 nm with a −3 dB bandwidth of 0.09 nm (= 40 GHz).

5. Discussion and conclusion

The obtained T-S conversion efficiency of 0.03% in our current setup is clearly too low to be considered as a viable solution for OTDM demultiplexing. In order to boost the conversion efficiency we propose to implement the SFG interaction in a PPLN planar waveguide, with the interacting waves confined in the vertical direction. The non-degenerate configuration utilized here and in [26] is ideally suited for this task, as it is impossible to use a non-collinear arrangement with vertical confinement in a planar waveguide. The advantages of performing the T-S conversion in a planar waveguide are twofold; the vertical mode height can be focused independently and more tightly thereby increasing the interaction intensity and the tight vertical mode does not impose any diffraction limitation as the mode is confined within the waveguide structure.

The estimated vertical mode size in a planar waveguide defined by titanium diffusion at the reference wavelength (1697 nm) is approximately 5.5μm ($1/e^2$ intensity points diameter). Compared to our current bulk PPLN crystal setup, where the vertical mode size of the reference beam is approximately 100 μm, this represents an intensity increase factor of 18, which should translate directly to a conversion efficiency improvement from the signal light to the generated SFG light. In addition, whereas the interaction length will still be limited by diffractive spreading in the non-confined horizontal direction, preservation of the beams' intensity in the vertical direction along the interaction length should result in a further

#175578 - $15.00 USD Received 5 Sep 2012; revised 27 Oct 2012; accepted 28 Oct 2012; published 19 Nov 2012

increase in conversion efficiency by a factor of √2. Thus a total increase by factor 25 in conversion efficiency as compared to the bulk PPLN T-S conversion reported here is expected due to these combined effects, bringing the overall conversion efficiency close to 1%.

In conclusion we have demonstrated high resolution and increased efficiency background-free time-to-space conversion using non-critically phase-matched SFG in a PPLN crystal. The quasi-monochromatic SFG output signal implies the potential for recovery of phase encoded information by coherent detection, allowing compatibility with advanced modulation formats such as n-QAM which are necessary for high spectral efficiency. We are currently planning a phase extraction experiment using a narrow linewidth local oscillator in order to demonstrate this possibility. The PPLN slab waveguide currently under fabrication will allow tight confinement of the light intensity in the vertical direction and thus further increase the conversion efficiency, en route towards practical time-to-space detection of optical waveforms in the lightwave telecommunication band.

Finally, the conversion of amplitude and, potentially, phase information from the time domain to the spatial domain by means of spectrally resolved SFG is a very general technique which can find applications in a number of fields in addition to optical communications. For example the ability to perform single-shot imaging of non-repetitive ultrafast temporal waveforms with high resolution would be useful for investigating femtosecond time scale molecular dynamics. T-S conversion may also be interesting for single wavelength channel real-time photonic analog-to-digital conversion due to the possibility for oversampling of the converted signal in the spatial domain, thus reducing detection errors.

#175578 - $15.00 USD Received 5 Sep 2012; revised 27 Oct 2012; accepted 28 Oct 2012; published 19 Nov 2012